CrossMark

MOLECULAR TOXICOLOGY

# Succinate dehydrogenase activity regulates PCB3-quinone-induced metabolic oxidative stress and toxicity in HaCaT human keratinocytes

**Wusheng Xiao · Ehab H. Sarsour · Brett A. Wagner · Claire M. Doskey · Garry R. Buettner · Frederick E. Domann · Prabhat C. Goswami**

**Abstract** Polychlorinated biphenyls (PCBs) and their metabolites are environmental pollutants that are known to have adverse health effects. 1-(4-Chlorophenyl)-benzo-2,5-quinone (4-ClBQ), a quinone metabolite of 4-monochlorobiphenyl (PCB3, present in the environment and human blood) is toxic to human skin keratinocytes, and breast and prostate epithelial cells. This study investigates the hypothesis that 4-ClBQ-induced metabolic oxidative stress regulates toxicity in human keratinocytes. Results from Seahorse XF96 Analyzer showed that the 4-ClBQ treatment increased extracellular acidification rate, proton production rate, oxygen consumption rate and ATP content, indicative of metabolic oxidative stress. Results from a q-RT-PCR assay showed significant increases in the mRNA levels of hexokinase 2 (*hk2*), pyruvate kinase M2 (*pkm2*) and glucose-6-phosphate dehydrogenase (*g6pd*), and decreases in the mRNA levels of succinate dehydrogenase (complex II) subunit C and D (*sdhc* and *sdhd*). Pharmacological inhibition of G6PD-activity enhanced the toxicity of 4-ClBQ, suggesting that the protective function of the pentose phosphate pathway is functional in 4-ClBQ-treated cells. The decrease in *sdhc* and *sdhd* expression was associated with a significant decrease in complex II activity and increase in mitochondrial levels of ROS. Overexpression of *sdhc* and *sdhd* suppressed 4-ClBQ-induced inhibition of complex II activity, increase in mitochondrial levels of ROS, and toxicity. These results suggest that the 4-ClBQ treatment induces metabolic oxidative stress in HaCaT cells, and while the protective function of the pentose phosphate pathway is active, inhibition of complex II activity sensitizes HaCaT cells to 4-ClBQ-induced toxicity.

**Keywords** PCB3-quinone · Polychlorinated biphenyls · Metabolic oxidative stress · Succinate dehydrogenase · G6PD · Glucose metabolism

## Abbreviations

| | |
|---|---|
| 4-ClBQ | 1-(4-Chlorophenyl)-benzo-2,5-quinone |
| 2-NBDG | 2-(*N*-(7-nitrobenz-2-oxa-1,3-diazol-4-yl) amino)-2-deoxyglucose |
| BSO | L-Buthionine sulfoximine |
| DHEA | Dehydroepiandrosterone |
| ECAR | Extracellular acidification rate |
| mBBr | Monobromobimane |
| METC | Mitochondrial electron transport chain |
| MFI | Mean fluorescence intensity |
| NBT | Nitro-blue tetrazolium chloride |
| OCR | Oxygen consumption rate |
| OXPHOS | Oxidative phosphorylation |
| PCBs | Polychlorinated biphenyls |
| PCB3 | 4-Monochlorobiphenyl |
| PEG-SOD | Polyethylene glycol-superoxide dismutase |
| PPP | Pentose phosphate pathway |
| PPR | Proton production rate |
| ROS | Reactive oxygen species |
| SDH | Succinate dehydrogenase |

W. Xiao · E. H. Sarsour · B. A. Wagner · C. M. Doskey · G. R. Buettner · F. E. Domann · P. C. Goswami (✉)
Free Radical and Radiation Biology Division, Department of Radiation Oncology, B180 Medical Laboratories, The University of Iowa, Iowa City, IA 52242, USA
e-mail: prabhat-goswami@uiowa.edu

## Introduction

Polychlorinated biphenyls (PCBs) are a class of persistent organic pollutants that have been used throughout the world

for industrial purposes due to their highly stable physical and chemical properties (Safe 1993). Because PCBs are hazardous to the environment and humans, commercial production and applications of PCBs were banned in the USA in 1979 (Ross 2004). Unfortunately, PCBs are ubiquitously found in the environment and biological organisms (Safe 1993; WHO 2003). Lower-chlorinated PCB congeners have been detected in air, old buildings, and human blood (Herrick et al. 2007, 2011; Liebl et al. 2004). PCBs are believed to cause a wide spectrum of adverse health effects including cancer (WHO 2003). The International Agency for Research on Cancer (IARC) very recently reclassified PCBs as Group 1 carcinogens (Lauby-Secretan et al. 2013).

4-Monochlorobiphenyl (PCB3), a lower-chlorinated and semi-volatile PCB congener, was found in human blood, Chicago air, soil, and commercial paints (DeCaprio et al. 2005; Hu and Hornbuckle 2009; Hu et al. 2010; Martinez et al. 2012). 1-(4-Chlorophenyl)-benzo-2,5-quinone (4-ClBQ) is a quinone metabolite of PCB3 (McLean et al. 1996). Previous results using electron paramagnetic resonance spectrometry have shown that 4-ClBQ generates semiquinone radicals in MCF-10A human mammary epithelial cells resulting in oxidative stress and toxicity (Venkatesha et al. 2008). Song et al. (2008, 2009) have demonstrated that PCB semiquinones and quinones produce reactive oxygen species (ROS: superoxide and hydrogen peroxide) via redox cycling and auto-oxidation. 4-ClBQ treatments have been shown to increase mitochondrial-generated ROS in human keratinocytes, and breast and prostate epithelial cells (Xiao et al. 2013; Zhu et al. 2009). Because mitochondria are the major organelles of cellular metabolism, these previously published results also suggest that cellular metabolism regulates PCB-induced adverse effects.

Cellular metabolism consists of glycolysis, the pentose phosphate pathway (PPP), and oxidative phosphorylation (OXPHOS). Glucose transporters import glucose into cells and hexokinase (HK) phosphorylates glucose into glucose-6-phosphate, which then proceeds through a series of glycolytic reactions resulting in the production of pyruvate (Lunt and Vander Heiden 2011). Glucose-6-phosphate is also metabolized through the PPP by glucose-6-phosphate dehydrogenase (G6PD) providing reducing equivalents (NADPH and GSH) and nucleotide precursor (ribose-5-phosphate) (Spitz et al. 2004; Wamelink et al. 2008). Under aerobic conditions, pyruvate is further metabolized through the tricarboxylic acid (TCA) cycle and OXPHOS. Initially, pyruvate is converted into acetyl-CoA by pyruvate dehydrogenase, which then initiates the TCA cycle producing electron carriers (NADH and $FADH_2$) in the mitochondrial matrix. NADH and $FADH_2$ transfer electrons through complex I, II, and III of the mitochondrial electron transport chain (MTEC) leading to the reduction of molecular oxygen at complex IV and generation of energy (ATP) at complex V (Balaban et al. 2005; Spitz et al. 2004). Cells coordinate these metabolic pathways in response to intracellular energy demand and extracellular stimuli as well as in response to oxidative insults.

Results from this study show that while the protective function of the PPP is functional, 4-ClBQ-induced toxicity in human keratinocytes results from a significant decrease in succinate dehydrogenase (complex II) activity.

## Materials and methods

### Chemicals, antibodies, and cell culture

4-ClBQ was provided by the Synthesis Core of the Iowa Superfund Research Project. 4-ClBQ was synthesized and purified as described previously (Lehmler and Robertson 2001). Dehydroepiandrosterone (DHEA), L-buthionine sulfoximine (BSO), nitro-blue tetrazolium chloride (NBT), disodium succinate, and polyethylene glycol-superoxide dismutase (PEG-SOD) were purchased from Sigma Chemical Co (St. Louis, MO). 2-(N-(7-nitrobenz-2-oxa-1,3-diazol-4-yl)amino)-2-deoxyglucose (2-NBDG), monobromobimane (mBBr), and MitoSOX Red were purchased from Molecular Probes (Eugene, OR). Human hexokinase 2 (HK2) and pyruvate kinase muscle 2 (PKM2) antibodies were obtained from Cell Signaling Technology (Danvers, MA); β-actin and c-myc antibodies were purchased from Santa Cruz Biotechnology (Santa Cruz, CA); glucose-6-phosphate dehydrogenase (G6PD) antibody was a generous gift from Dr. Netanya Y. Spencer, Department of Anatomy and Cell Biology, University of Iowa.

Spontaneously immortalized human skin keratinocytes (HaCaT) obtained from Dr. Norbert Fusenig (German Cancer Research Center, Heidelberg, Germany) (Boukamp et al. 1988) were cultured in Dulbecco's modified Eagle's medium (DMEM) with 10 % fetal bovine serum at 37 °C in a 5 % $CO_2$ atmosphere. Dimethyl sulfoxide (DMSO) was used to prepare stock solutions of 4-ClBQ (Venkatesha et al. 2008). 4-ClBQ treatments were carried out in serum-free DMEM for 24 h followed by the addition of serum-containing regular medium. The concentration of 0.1–3.0 μM of PCB used in this study is based on a previous report of 0.003–6.5 μM PCBs that were detected in the blood of individuals living in Anniston, Alabama (Hansen et al. 2003). A clonogenic assay and flow cytometry analysis of propidium iodide-stained cells were used to measure cell survival (Venkatesha et al. 2008; Zhu et al. 2009).

### Flow cytometry assays

Glucose uptake assay: $2 \times 10^5$ cells were seeded and treated with 0–3.0 μM 4-ClBQ for 24 h. Monolayer cultures were

washed twice and incubated with DMEM containing glucose (1 g L$^{-1}$) and 2-NBDG (20 μM) for 1 h. 2-NBDG uptake was measured using BD LSRII cytometer (excitation at 465 nm, emission at 540 nm) (Zou et al. 2005). The mean fluorescence intensity (MFI) of 20,000 cells was analyzed for each sample and corrected for autofluorescence. Fold change in MFI of 4-ClBQ-treated cells was calculated relative to the MFI of cells that were not treated with 4-ClBQ.

Cellular thiol content: Control and 4-ClBQ-treated cells were trypsinized and incubated with 50 nM mBBr for 10 min. BD LSRII cytometer was used to measure mBBr fluorescence; excitation at 405 nm and emission at 450 nm (Cossarizza et al. 2009). The specificity of mBBr to the measurement of cellular GSH was determined by treating cells with 100 μM BSO prior to the mBBr assay. The MFI of 20,000 cells was analyzed for each sample and corrected for autofluorescence. The MFI of BSO-treated cells was subtracted from each sample, and fold change was calculated relative to the MFI of cells that were not treated with 4-ClBQ.

Cellular ROS levels: Control and 4-ClBQ-treated cells were incubated with 2 μM MitoSOX Red, and MitoSOX oxidation was measured following a previously published protocol (Xiao et al. 2013; Zhu et al. 2009). The specificity of the assay for the measurements of ROS was determined by repeating the assay in cells treated with 100 U mL$^{-1}$ PEG-SOD. Becton–Dickinson FACScan flow cytometer was used to measure MitoSOX oxidation; excitation 488 nm and emission 585 nm. The MFI of 10,000 cells was analyzed for each sample and corrected for autofluorescence. Fold change in MFI of 4-ClBQ-treated cells was calculated relative to the MFI of cells that were not treated with 4-ClBQ.

## Immunoblotting

Total protein lysates were separated on 12 % SDS-PAGE and electroblotted to nitrocellulose membrane. Immunoblotting was performed using antibodies to human HK2 (1:1,000), PKM2 (1:1,000), G6PD (1:1,000), and c-myc (1:200). Pierce ECL Plus reagent (Thermo Scientific, Rockford, IL) and Typhoon FLA 7000 (GE Healthcare, Waukesha, WI) were used for visualization of immune-reactive polypeptides. Images were quantitated using ImageJ software. Fold change was calculated after correction for loading (actin levels) in each sample and relative to cells that were not treated with 4-ClBQ.

## cDNA synthesis and quantitative RT-PCR assay

Total RNA was extracted using TRIzol (Invitrogen, Carlsbad, CA). ND1000 Nanodrop spectrophotometer (Nanodrop,

Wilmington, DE) was used to measure the concentration and purity of RNA. One microgram of RNA was reverse transcribed using the cDNA Archive Kit (Applied Biosystems, Carlsbad, CA). Real-time PCR amplification was performed using primer pair for individual genes (Suppl. Table 1), Power SYBR Green and StepOnePlus™ System (Applied Biosystems, Carlsbad, CA). Changes in mRNA levels were calculated as follows:

$$\Delta\Delta C_t = \Delta C_t(\text{4-ClBQ-treated cells}) - \Delta C_t(\text{control cells});$$
$$\text{relative expression} = 2^{-\Delta\Delta C_t}$$

## Metabolic flux measurements

Extracellular acidification rate (ECAR), proton production rate (PPR), and oxygen consumption rate (OCR) were measured using Seahorse XF96 Extracellular Flux Analyzer following manufacturer supplied protocol (Seahorse Bioscience, Billerica, MA). Briefly, HaCaT cells were plated in Seahorse XF96 cell culture microplates at a density of $1 \times 10^4$ cells per well and treated with 0–3.0 μM 4-ClBQ. Culture medium was replaced with pre-warmed Seahorse MEM medium (pH = 7.4) containing 25 mM glucose and 1 mM sodium pyruvate, and cells were incubated in $CO_2$-free incubator for 1 h. ECAR, PPR, and OCR were measured using the XF96 instrument; cell number in individual wells was counted using a hemocytometer. Rates were calculated per cell for control and each treatment.

## Complex II activity assay

A cell-based assay (Zhang et al. 2013) with minor modification was used to measure Complex II activity. Monolayer cultures of control and 24-h 4-ClBQ-treated HaCaT cells were air-dried and incubated with 0.55 mM NBT and 0.05 M disodium succinate at 37 °C overnight. Cultures were stained with Hoechst to visualize nuclei. Olympus CKX41 microscope (Olympus, Tokyo, Japan) and ImageJ software were used to quantitate results. The integrated density of each image was normalized to the number of nuclei in that field. One thousand nuclei in each treatment group were analyzed, and fold change in complex II activity was calculated relative to complex II activity of cells that were not treated with 4-ClBQ.

## Cellular ATP content

CellTiter-Glo® Luminescent Cell Viability Assay kit (Promega, Madison, WI) was used to measure cellular ATP content following the manufacturer supplied protocol. Control and 4-ClBQ-treated cells were counted using a Z1 Coulter Counter (Beckman Coulter, Fullerton,

CA), and cell number of each sample was adjusted to $5 \times 10^5$ cells mL$^{-1}$. Hundred microliters of cell suspension and 100 μL of CellTiter-Glo reagent were added into each well of an opaque-walled 96-well plate. Luminescence was recorded using a luminometer. A standard curve was used to calculate levels of ATP in each sample.

### SDHC and SDHD overexpression

TrueORFGold expression-validated cDNA clones of pCMV6-entry, Myc-DDK-tagged human SDHC, and Myc-DDK-tagged human SDHD were purchased from OriGene (Rockville, MD). HaCaT cells were cultured to 70–80 % confluence and then transfected with Empty (pCMV6-entry), and complex II SDHC and SDHD cDNA containing plasmid DNAs (Myc-DDK-SDHC and Myc-DDK-SDHD) using Lipofectamine 3000 (Life Technologies, Grand Island, NY). Transfected cells were subcultured and treated with 4-ClBQ for 24 h. A q-RT-PCR assay was used to measure *sdhc* and *sdhd* mRNA expression. Immunoblotting of c-myc-tag was used to measure protein levels of SDHC and SDHD.

### Statistical analysis

One-way analysis of variance (ANOVA) followed by Tukey post test (SPSS 21.0 software) was performed to evaluate statistical significance of results. Results are presented as mean ± SD. Results from at least $n = 3$ with $p < 0.05$ were considered as significant.

## Results

### 4-ClBQ treatment induces metabolic oxidative stress in HaCaT cells

In this study, we used HaCaT human keratinocytes because skin is one of the target tissues for exposure to airborne PCBs. Previous studies report that 4-ClBQ treatment increases mitochondrial ROS levels in human keratinocytes, breast, and prostate epithelial cells resulting in toxicity (Xiao et al. 2013; Zhu et al. 2009). Because mitochondria are the major organelles for cellular metabolism, results from these previous studies also suggest that cellular metabolism regulates some aspects of PCB-induced adverse cellular effects. In fact, PCB153 treatment increased glucose consumption in MCF-10A human breast epithelial cells (Venkatesha et al. 2010). To determine whether 4-ClBQ treatment induces metabolic oxidative stress in HaCaT cells, initially glucose uptake was measured in control and 4-ClBQ-treated cells using glucometer and flow cytometry-based assays. Results using the glucometer

showed approximately 400 amol cell$^{-1}$ s$^{-1}$ glucose uptake in control cells, which increased to approximately 600 amol cell$^{-1}$ s$^{-1}$ in 1.0 μM and 1,000 amol cell$^{-1}$ s$^{-1}$ in 3.0 μM 4-ClBQ-treated cells (Fig. 1a). 4-ClBQ-induced increase in glucose uptake was also observed from the flow cytometry assay. Control and 4-ClBQ-treated cells were incubated with 2-NBDG, and fluorescence was measured using flow cytometry. Representative histograms are shown in Fig. 1b (left panel), and results obtained from 20,000 cells are shown in Fig. 1b (right panel). Consistent with the results obtained from the glucometer, results from the flow cytometry assay showed approximately twofold increase in glucose uptake in 4-ClBQ-treated cells compared to glucose uptake in untreated cells.

To further investigate the hypothesis of metabolic oxidative stress regulating 4-ClBQ-induced toxicity, Seahorse XF96 Analyzer was used to measure ECAR and PPR. Changes in ECAR and PPR in 4-ClBQ-treated cells are indicative of changes in glycolysis rate induced by the 4-ClBQ treatment. The ECAR in untreated cells was measured to be approximately 8 npH cell$^{-1}$ s$^{-1}$ (Fig. 1c; Suppl. Figure 1a). 4-ClBQ treatment showed a dose-dependent increase in ECAR: 14 npH cell$^{-1}$ s$^{-1}$ and 18 npH cell$^{-1}$ s$^{-1}$ in 1.0 and 3.0 μM 4-ClBQ-treated cells, respectively (Fig. 1c; Suppl. Figure 1a). Consistent with these results, 4-ClBQ treatment resulted in a dose-dependent increase in PPR: approximately 150 amol H$^+$ cell$^{-1}$ s$^{-1}$ in untreated cells compared to 300 amol H$^+$ cell$^{-1}$ s$^{-1}$ and 380 amol H$^+$ cell$^{-1}$ s$^{-1}$ in 1.0 and 3.0 μM 4-ClBQ-treated cells, respectively (Fig. 1d; Suppl. Figure 1b). These results suggest that the 4-ClBQ-induced metabolic oxidative stress could be due to an increase in glucose uptake and glycolytic rate.

### The protective function of the pentose phosphate pathway is functional in 4-ClBQ-treated cells

In general, oxidative stress-induced increase in glucose consumption is believed to be a protective response of cells to counter oxidative insults. To determine whether the increase in ECAR and PPR in 4-ClBQ-treated HaCaT cells (Fig. 1) could be due to changes in the expression of specific glucose metabolism genes, human glucose metabolism PCR arrays (SABiosciences) were used to measure mRNA levels of 84 metabolic genes in control and 4-ClBQ-treated cells (data not shown). A quantitative RT-PCR assay was used to further verify the results that were obtained from the PCR arrays. Results showed statistically significant increase in the expression of hexokinase 2 (*hk2*), pyruvate kinase muscle 2 (*pkm2*), and glucose-6-phosphate dehydrogenase (*g6pd*), while there was no change in the mRNA levels of phosphofructokinase 1 (*pfk1*), pyruvate kinase muscle 1 (*pkm1*), and lactate dehydrogenase A (*ldha*) (Fig. 2a). The mRNA and protein levels of *hk2*, *pkm2*, and
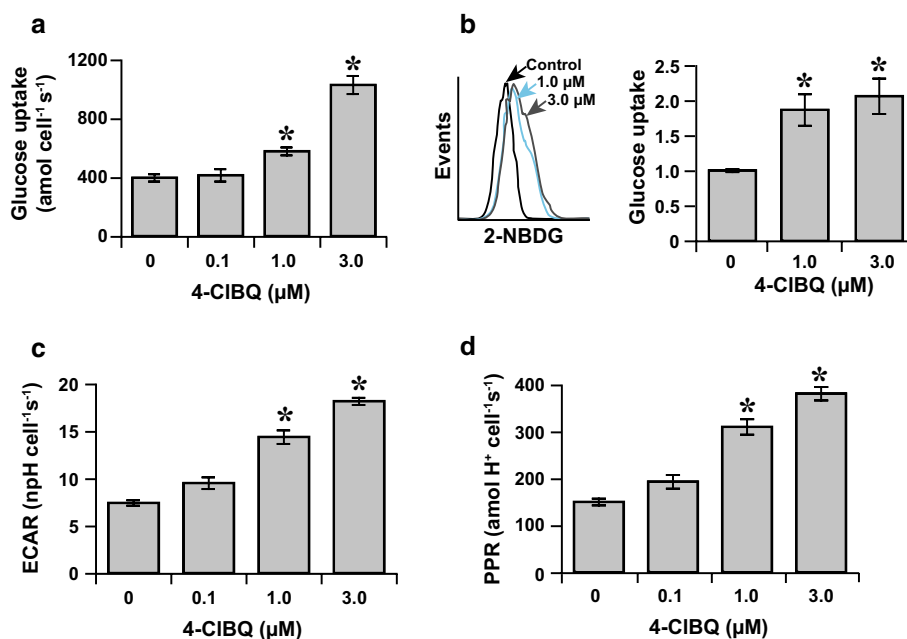
**Fig. 1** 4-ClBQ treatment enhances glucose uptake and glycolytic rate in HaCaT cells. **a, b** Glucose uptake increased significantly in 4-ClBQ-treated cells. **a** Glucose uptake was measured in untreated and 24-h 4-ClBQ-treated HaCaT cells using a Bayer Glucometer Elite with Bayer Ascensia Elite Blood glucose test strips as previously described (Venkatesha et al. 2010). *Asterisks* represent statistical significance compared to untreated cells; $p < 0.05$, $n = 3$. **b** A flow cytometry-based assay was used to measure glucose uptake in untreated and 24-h 4-ClBQ-treated cells. Monolayer cultures of control and 4-ClBQ-treated cells were incubated with 20 μM 2-NBDG, and fluorescence was measured using BD LSRII flow cytometer: *left panel* representative histograms of 2-NBDG fluorescence; *right panel* fold change in mean fluorescence intensity was calculated relative to untreated cells. *Asterisks* represent statistical significance compared to untreated cells; $p < 0.05$, $n = 3$. **c, d** Significant increase in the extracellular acidification rate (ECAR) and proton production rate (PPR) in 4-ClBQ-treated cells. ECAR and PPR in untreated and 4-ClBQ-treated cells were measured by using the Seahorse XF96 Analyzer following manufacturer supplied protocols; rates were calculated per cell. *Asterisks* represent statistical significance compared to untreated cells; $p < 0.05$, $n = 3$

*g6pd* were further examined in cells treated with 0–3.0 μM 4-ClBQ. Results showed a dose-dependent increase in the mRNA and protein levels of *hk2*, *pkm2*, and *g6pd* (Fig. 2 b–d). These results suggest that an increase in the expression of a subset of the glucose metabolism genes may account for the increases in the ECAR and PPR that were observed in the 4-ClBQ-treated cells.

4-ClBQ treatment-induced increase in the expression of *g6pd* suggests that cells activate the PPP shunt to counter 4-ClBQ-induced metabolic oxidative stress and toxicity. Because G6PD is the rate-limiting step of the PPP and PPP influences cellular redox state, an increase in the expression of *g6pd* is anticipated to shift the cellular redox state to a more reducing environment. A reducing environment is anticipated to suppress 4-ClBQ-induced metabolic oxidative stress and toxicity, while inhibiting the PPP is anticipated to augment 4-ClBQ-induced toxicity. A flow cytometry assay was used to determine whether the 4-ClBQ treatment-induced increase in the expression of *g6pd* (Fig. 2d) impacts intracellular GSH content. Untreated and 4-ClBQ-treated cells were incubated with 50 nM mBBr, and fluorescence was analyzed by flow cytometry. The specificity of the assay for measurements of intracellular GSH content was determined by incubating cells with 100 μM BSO prior to the addition of mBBr. A shift to the right in the representative histogram (Fig. 3a, left panel) indicates that the 4-ClBQ treatment increased the fluorescence of mBBr suggesting an increase in intracellular total thiol content. A shift to the left in the representative histogram (Fig. 3a, left panel) in BSO-treated cells indicates the specificity of the assay for measurements of intracellular GSH content. BSO inhibits *de novo* synthesis of GSH. The MFI of mBBr collected from 20,000 BSO-treated cells was subtracted from the MFI of mBBr in control and 4-ClBQ-treated cells, and fold change in MFI of mBBr in 4-ClBQ-treated cells was calculated relative to the MFI of cells not treated with 4-ClBQ. Results showed mBBr fluorescence was approximately threefold in 1.0 μM and more than fourfold in 3.0 μM 4-ClBQ-treated cells (Fig. 3a, right panel). These results show that the 4-ClBQ-induced increase in the expression of *g6pd* was also associated with a significant increase in intracellular GSH content.

To determine whether the 4-ClBQ-induced increase in the expression of *g6pd* protects HaCaT cells from

4-ClBQ-induced toxicity, cells were incubated with 100 μM DHEA (inhibits G6PD activity) for 24 h prior to the 4-ClBQ treatment. A clonogenic assay was used to determine cell survival (Fig. 3b). Consistent with our previously published results (Xiao et al. 2013), cell survival decreased significantly in 4-ClBQ-treated cells: approximately 50 % in 1.0 μM and 70 % in 3.0 μM 4-ClBQ-treated cells (Fig. 3b, right panel). Prior treatment with DHEA augmented 4-ClBQ-induced toxicity: approximately 70 % decrease in survival in 1.0 μM and 90 % decrease in survival in 3.0 μM 4-ClBQ-treated cells (Fig. 3b, right panel). Comparable results were also obtained from toxicity measurements using flow cytometry analysis of propidium iodide-stained positive (indicative of dead cells) and negative (indicative of live cells) cells (data not shown). Taken together, these results suggest that the protective function of the PPP is active in 4-ClBQ-treated HaCaT cells.

Complex II activity regulates 4-ClBQ-induced mitochondrial oxidative stress and toxicity in HaCaT cells

Although the protective function of the PPP is active in 4-ClBQ-treated cells, these cells still demonstrate significant toxicity. This prompted us to determine whether mitochondrial oxidative stress mediates toxicity in 4-ClBQ-treated cells. Toward this objective, initially OCR was measured in control and 4-ClBQ-treated cells using the Seahorse XF96 Analyzer. The OCR in control cells was found to be approximately 20 amol $O_2$ cell$^{-1}$ s$^{-1}$ which increased to approximately 30 amol $O_2$ cell$^{-1}$ s$^{-1}$ in 4-ClBQ-treated cells (Fig. 4a; Suppl. Figure 1c). Consistent with the increase in the OCR, cellular ATP levels increased from approximately 4 fmol cell$^{-1}$ in control to approximately 6 fmol cell$^{-1}$ in 4-ClBQ-treated cells (Fig. 4b). These results suggest that the 4-ClBQ treatment induces mitochondrial oxidative stress in HaCaT cells.

To further investigate whether the 4-ClBQ-induced mitochondrial oxidative stress is due to a change in the expression of specific genes regulating mitochondrial metabolism, a q-RT-PCR assay was used to assess the expression of mitochondrial metabolism genes that were selected based on the results from the glucose metabolism PCR arrays (data not shown) and literature reports. Whereas the levels of mRNA (Fig. 4c) and protein (data not shown) of the majority of these genes were not affected by the 4-ClBQ treatment, approximately a twofold decrease in the expression of *sdhc* and *sdhd* was observed in 4-ClBQ-treated cells (Fig. 4c). The decrease in the expression of complex II subunit *sdhc* and *sdhd* was also evident in cells treated with different concentrations of 4-ClBQ (Fig. 5a).
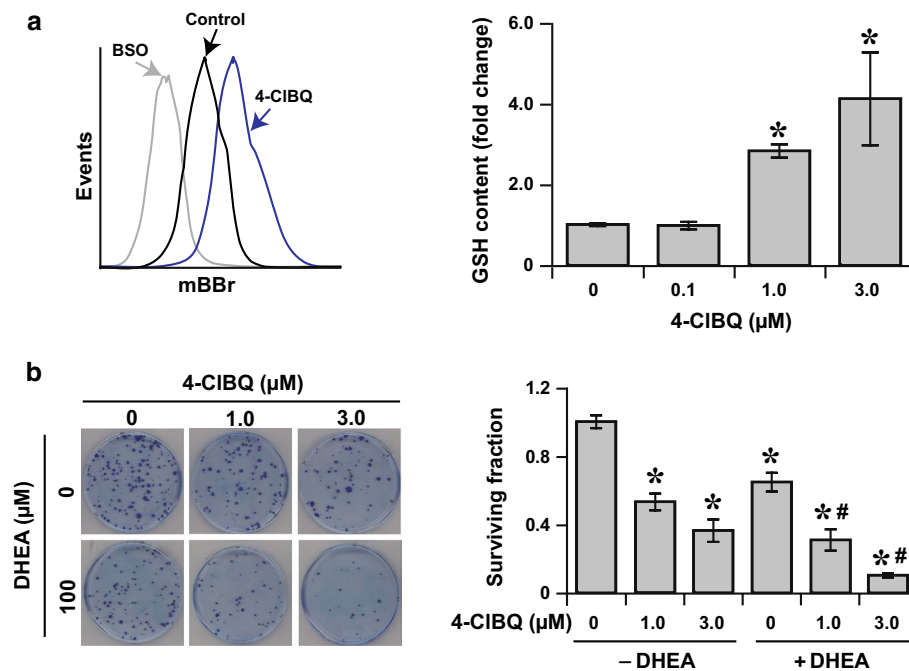
**Fig. 3** Inhibition of G6PD activity sensitizes HaCaT cells to 4-ClBQ-induced toxicity. **a** 4-ClBQ treatment increases cellular GSH content. Monolayer cultures of control and 24-h 4-ClBQ-treated cells were incubated with 50 nM mBBr and fluorescence measured by flow cytometry. The specificity of the assay for measurements of cellular GSH content was determined by incubating cells with 100 μM BSO prior to incubation with mBBr. *Left panel* representative histograms of control, BSO, and 3.0 μM 4-ClBQ-treated cells. *Right panel* mean fluorescence intensity, *MFI* of BSO-treated cells was subtracted from MFI of control and 4-ClBQ-treated cells and fold change calculated relative to the MFI of untreated cells. *Asterisks* represent statistical significance compared to untreated cells; $p < 0.05$, $n = 3$. **b** Pharmacological inhibition of G6PD activity sensitizes HaCaT cells to 4-ClBQ-induced toxicity. Monolayer cultures were incubated with 100 μM DHEA prior to incubation with 4-ClBQ. A clonogenic assay was used to measure cell survival. *Left panel* representative dishes with colonies of control, DHEA, and 4-ClBQ-treated cells; *right panel* surviving fraction was calculated relative to untreated cells. *Asterisks* represent statistical significance compared to untreated cells; [#]Significance compared to 4-ClBQ treatment in absence of DHEA; $p < 0.05$, $n = 3$

Interestingly, the same treatment did not affect expression of complex II subunit *sdha* and *sdhb* (Fig. 5a). A cell-based assay (Zhang et al. 2013) was used to determine whether the 4-ClBQ-induced decrease in the expression of *sdhc* and *sdhd* impacts complex II activity (Fig. 5b). Results showed that 4-ClBQ-induced decrease in the expression of complex II subunit *sdhc* and *sdhd* was also associated with a more than 60 % decrease in complex II activity (Fig. 5b, lower panel). These results suggest that 4-ClBQ treatment induces mitochondrial oxidative stress and toxicity probably by suppressing the activity of complex II.

To determine the causality of complex II activity regulating 4-ClBQ-induced mitochondrial oxidative stress and toxicity, additional experiments were performed in *sdhc* and *sdhd* overexpressing cells. HaCaT cells were transfected with plasmid DNAs carrying human *sdhc* and *sdhd* cDNAs, and transgene expression was measured using q-RT-PCR, Western blotting, and activity assays. Results from the q-RT-PCR assay showed approximately fourfold increase in the mRNA levels of *sdhc* and tenfold increase in the mRNA levels of *sdhd* (Fig. 6a). Because *sdhc* and

*sdhd* were tagged with c-myc, Western blotting analysis of c-myc was used to assess protein levels of exogenously expressed SDHC and SDHD. Consistent with the mRNA data, overexpression of *sdhc* and *sdhd* resulted in an increase in their protein levels (Fig. 6b). The cell-based assay (Fig. 5b) was used to measure complex II activity in 4-ClBQ-treated control and *sdhc/sdhd* overexpressing cells (Fig. 6c). As shown before (Fig. 5b), 4-ClBQ treatment decreased complex II activity approximately 30 % in cells transfected with a control plasmid DNA (Fig. 6c). However, cells overexpressing *sdhc/sdhd* were protected from the 4-ClBQ-induced decrease in complex II activity (Fig. 6c). Next, it was determined whether overexpression of *sdhc/sdhd* affects 4-ClBQ-induced increase in levels of mitochondrial ROS. Control and *sdhc/sdhd* overexpressing cells were treated with 4-ClBQ and incubated with Mito-SOX. MitoSOX oxidation was measured using flow cytometry. As reported previously (Xiao et al. 2013), 4-ClBQ treatment significantly increased MitoSOX oxidation in cells transfected with a control plasmid DNA (Fig. 6d, e). Interestingly, such an increase in MitoSOX oxidation was
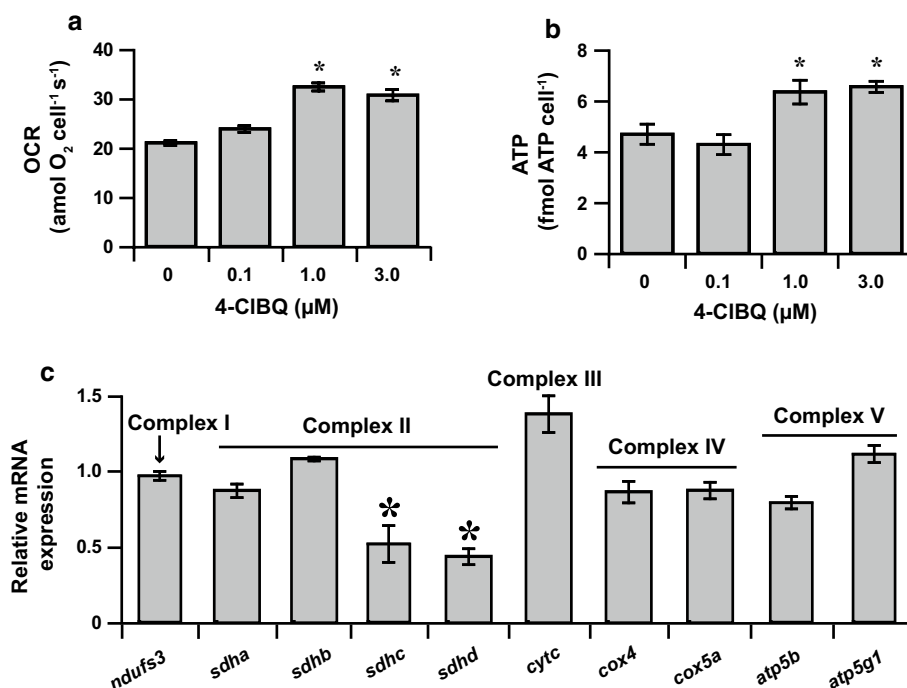
**Fig. 4** 4-ClBQ treatment perturbs mitochondrial metabolism. **a, b** A significant increase in OCR and ATP levels was observed in 4-ClBQ-treated cells. **a** OCR in control and 4-ClBQ-treated cells was measured using Seahorse XF96 Analyzer following manufacturer supplied protocol. *Asterisks* represent statistical significance compared to untreated cells; $p < 0.05$, $n = 3$. **b** ATP content in control and 4-ClBQ-treated cells were measured using CellTiter-Glo® Luminescent Cell Viability Assay kit. The luminescence of $5 \times 10^4$ cells of each sample was measured, and ATP content was calculated using a standard curve. *Asterisks* represent statistical significance compared to untreated cells; $p < 0.05$, $n = 3$. **c** A significant down-regulation of mRNA expression of succinate dehydrogenase (Complex II) subunit C and D in 4-ClBQ-treated cells. A quantitative RT-PCR assay was used to measure mRNA expression of selected genes related to the mitochondrial electron transport chain in control and 3.0 μM 4-ClBQ-treated cells. Fold change was calculated relative to individual mRNA expression in untreated cells. *Asterisks* represent statistical significance compared to individual mRNA expression in untreated cells; $p < 0.05$, $n = 3$

significantly suppressed in 4-ClBQ-treated *sdhc/sdhd* over-expressing cells (Fig. 6d, e). Results from a clonogenic assay showed approximately 20 % cell death in 1.0 μM 4-ClBQ-treated cells transfected with a control plasmid DNA (Fig. 6f). However, the same treatment resulted in only 7 % cell death in *sdhc/sdhd* overexpressing cells. Overall, these results suggest that complex II activity regulates 4-ClBQ-induced mitochondrial oxidative stress and toxicity in HaCaT cells.

## Discussion

PCBs are environmental pollutants that have been recently classified as Group 1 carcinogens (Lauby-Secretan et al. 2013). PCB3 has been detected in air and human blood (DeCaprio et al. 2005; Hu et al. 2010). Cytochrome P450 enzymes metabolize PCB3 to its hydroxylated form, which further undergoes a second hydroxylation reaction resulting in PCB3 hydroquinone and quinone (McLean et al. 1996). 4-ClBQ, a quinone metabolite of PCB3 induces oxidative

stress and toxicity in human keratinocytes, and breast and prostate epithelial cells (Venkatesha et al. 2008; Xiao et al. 2013; Zhu et al. 2009). Results from this study show that the 4-ClBQ treatment increases glucose and oxygen consumption rates, and decreases complex II activity. While the protective properties of the pentose phosphate pathway are functional in 4-ClBQ-treated cells, 4-ClBQ-induced down-regulation of complex II activity results in metabolic oxidative stress and toxicity in HaCaT cells (Fig. 7). These results support the hypothesis that complex II activity regulates PCB3-quinone-induced metabolic oxidative stress and toxicity in HaCaT.

Previous studies report the formation of a semiquinone radical from oxygenated PCBs (Song et al. 2008; Venkatesha et al. 2008). Electron paramagnetic resonance spectroscopy measurements detected a singlet peak at $g = 2.005$ in 4-ClBQ-treated MCF10A human breast epithelial cells indicating the formation of a semiquinone radical; no such signal was detected in control cells that were not treated with 4-ClBQ (Venkatesha et al. 2008). Semiquinone radicals are believed to be the primary source for the formation
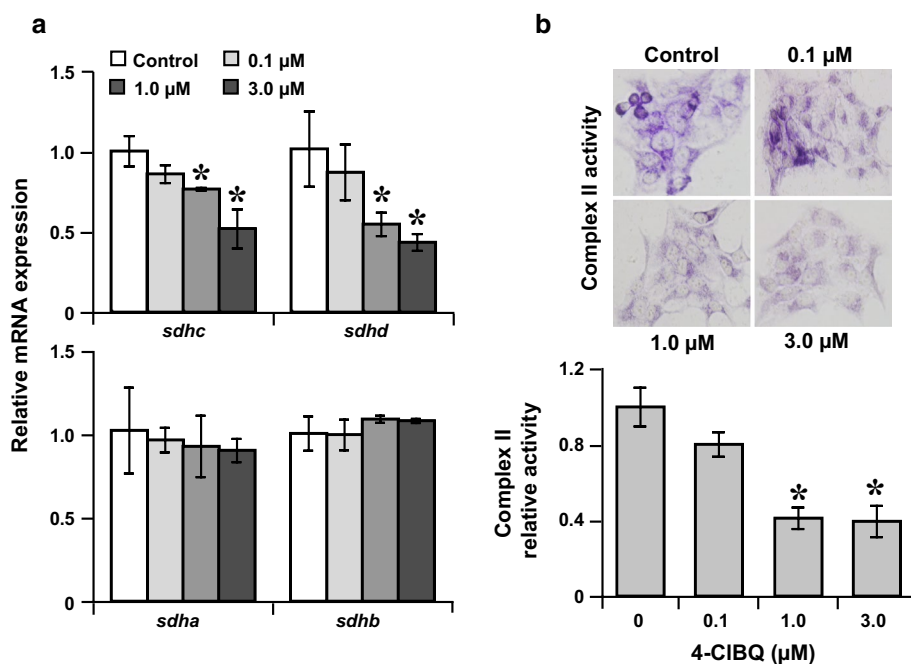
**Fig. 5** 4-ClBQ treatment decreases complex II activity. **a** A dose-dependent decrease in mRNA expression of *sdhc* and *sdhd* in 4-ClBQ-treated cells. A q-RT-PCR assay was performed to measure mRNA expression of *sdha*, *sdhb*, *sdhc*, and *sdhd* in control and 4-ClBQ-treated cells. Fold change was calculated relative to mRNA expression in untreated cells; *asterisks* represent statistical significance compared to untreated cells; $p < 0.05$, $n = 3$. **b** A dose-dependent decrease in complex II activity in 4-ClBQ-treated cells. A cell-based assay (Zhang et al. 2013) was used to measure complex II

activity in control and 4-ClBQ-treated cells. *Upper panel* representative microscopy images of cells showing complex II activity (purple color; magnification: ×400); *lower panel* purple color fluorescence intensity in the microscopy images was quantitated and normalized to the number of nuclei in each image using ImageJ software. A total number of 1,000 nuclei from three different dishes were scored in each treatment group. Fold change was calculated relative to untreated cells; *asterisks* represent statistical significance compared to untreated cells; $p < 0.05$, $n = 3$

of ROS from the PCB hydroquinone/quinone redox system (Song et al. 2008, 2009). Previous studies also report an increase in the levels of mitochondrial ROS in 4-ClBQ-treated human keratinocytes, and breast and prostate epithelial cells (Xiao et al. 2013; Zhu et al. 2009). Additional studies are needed to investigate how autoxidation and redox cycling of 4-ClBQ increase the steady-state levels of mitochondrial ROS. However, because mitochondria are the major organelles of cellular metabolism, 4-ClBQ-induced increase in the levels of mitochondrial ROS (Fig. 6; Xiao et al. 2013) also suggests that the 4-ClBQ treatment induces metabolic oxidative stress.

Cellular metabolism (glycolysis, PPP, TCA cycle and OXPHOS) is evolved to convert glucose into carbon dioxide and water, while maximizing the production of energy (ATP) and providing biosynthetic intermediates (nucleotides) as well as reducing equivalents (GSH and NADPH). Increased glucose metabolism in response to oxidative stress is believed to generate reducing equivalents (GSH and NADPH) to detoxify hydroperoxides. Consistent with this notion, a dose-dependent increase in glucose uptake was observed in 4-ClBQ-treated HaCaT cells (Fig. 1a, b). The increase in glucose uptake in 4-ClBQ-treated cells

was also associated with a significant increase in ECAR and PPR (Fig. 1c, d; Suppl. Figure 1a, b). PCB-induced increase in glucose uptake was also observed earlier in PCB153-treated MCF10A human breast epithelial cells (Venkatesha et al. 2010). PCB126 treatment has been reported to suppress forskolin-induced gluconeogenesis in primary mouse hepatocytes (Zhang et al. 2012). These previously published reports and results presented in Fig. 1 indicate that PCB exposure perturbs glucose metabolism.

Glucose metabolism is a multi-step process. To investigate the molecular pathways involved in 4-ClBQ-induced increases in glucose metabolism, human glucose metabolism PCR arrays and q-RT-PCR assays were performed. While the mRNA expression of the majority of the glucose metabolism genes was not affected by the 4-ClBQ treatment (data not shown), a significant increase in the mRNA levels of *hk2*, *pkm2*, and *g6pd* was observed (Fig. 2a). 4-ClBQ treatment showed a dose-dependent increase in the mRNA and protein levels of HK2, PKM2, and G6PD (Fig. 2b–d). Both HK2 and PKM2 are the regulatory enzymes catalyzing irreversible steps of glycolysis. HK2 catalyzes the first step of glycolysis by phosphorylating glucose at carbon 6 into glucose-6-phosphate; and PKM2
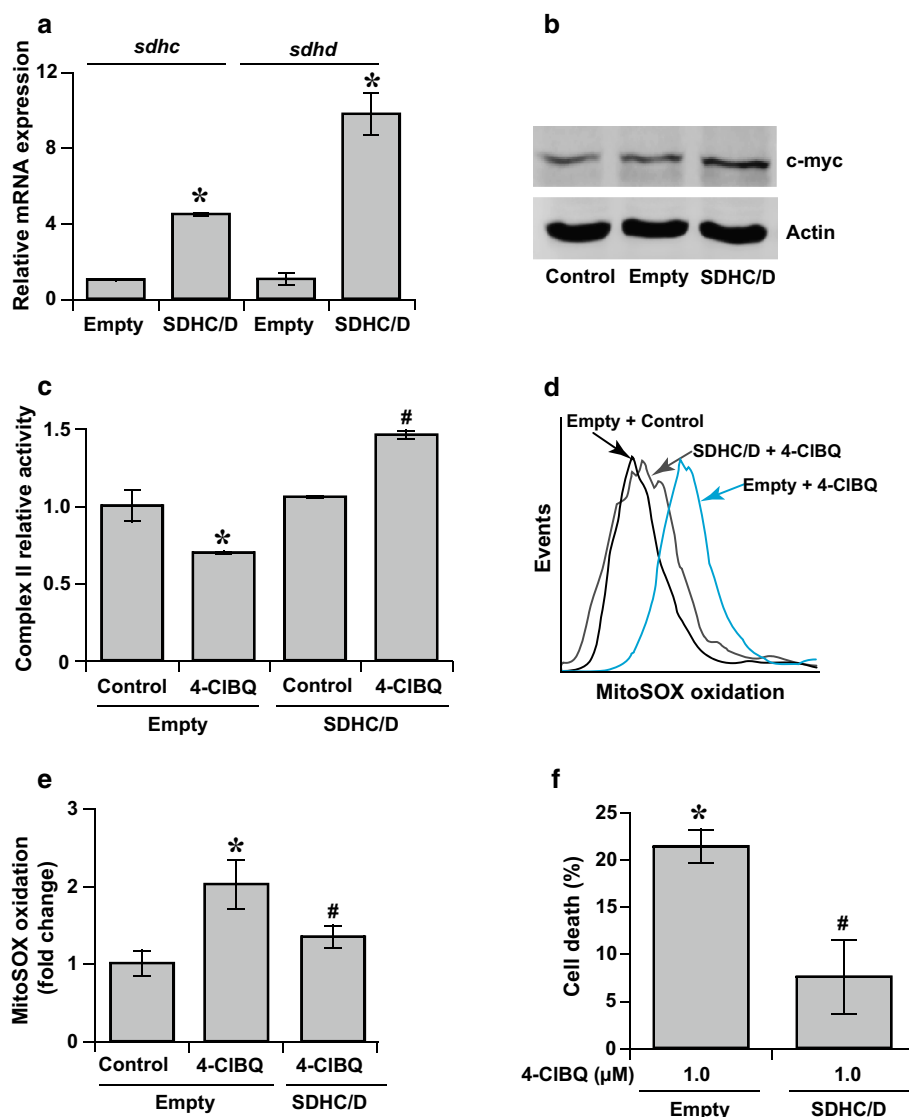
**Fig. 6** Complex II activity regulates metabolic oxidative stress and toxicity in 4-ClBQ-treated HaCaT cells. **a**, **b** Overexpression of *sdhc* and *sdhd* following transient transfection of cells. HaCaT cells were transfected with TrueORFGold expression-validated cDNA clones of pCMV6-entry (*Empty*), and Myc-DDK-tagged human SDHC and SDHD plasmid DNAs (OriGene, Rockville, MD). Transgene expression in cells transfected with Empty plasmid DNA and cells co-transfected with SDHC and SDHD plasmid DNAs was verified using q-RT-PCR (**a**) and Western blotting (**b**) assays. Fold change in mRNA expression was calculated relative to mRNA levels in Empty-plasmid-DNA-transfected cells. *Asterisks* represent statistical significance compared to Empty-plasmid-DNA-transfected cells; $p < 0.05$, $n = 3$. **c** 4-ClBQ-induced decrease in complex II activity is suppressed in cells overexpressing SDHC and SDHD. A cell-based assay (Fig. 5b) was used to measure complex II activity in Empty- and SDHC-SDHD-plasmid-DNA-transfected cells that were incubated with and without 1.0 μM 4-ClBQ. *Asterisk* represents statistical significance compared to Empty-plasmid-transfected cells that were not treated with 4-ClBQ; #Significance compared to 4-ClBQ-

treated cells; $p < 0.05$, $n = 3$. **d**, **e** 4-ClBQ-induced increase in the levels of mitochondrial ROS is suppressed in cells overexpressing SDHC and SDHD. Control and 1.0 μM 4-ClBQ-treated Empty- and SDHC-SDHD-plasmid-DNA-transfected cells were incubated with MitoSOX Red and MitoSOX-Red oxidation was measured using flow cytometry. Representative histograms of MitoSOX-Red fluorescence (**d**) and fold change in mean fluorescence intensity were calculated relative to Empty-plasmid-transfected cells that were not treated with 4-ClBQ (**e**). *Asterisk* represents statistical significance compared to Empty-plasmid-transfected cells that were not treated with 4-ClBQ; #Significance compared to 4-ClBQ-treated Empty-plasmid-transfected cells; $p < 0.05$, $n = 3$. **f** Complex II activity regulates 4-ClBQ-induced toxicity. A clonogenic assay was used to measure toxicity in 1.0 μM 4-ClBQ-treated Empty- and SDHC-SDHD-plasmid-DNA-transfected cells. *Asterisk* represents statistical significance compared to cells without 4-ClBQ treatment; #Significance compared to 4-ClBQ-treated Empty-plasmid-DNA-transfected cells; $p < 0.05$, $n = 3$

**Fig. 7** Proposed mechanisms of 4-ClBQ-induced metabolic oxidative stress and toxicity in HaCaT cells
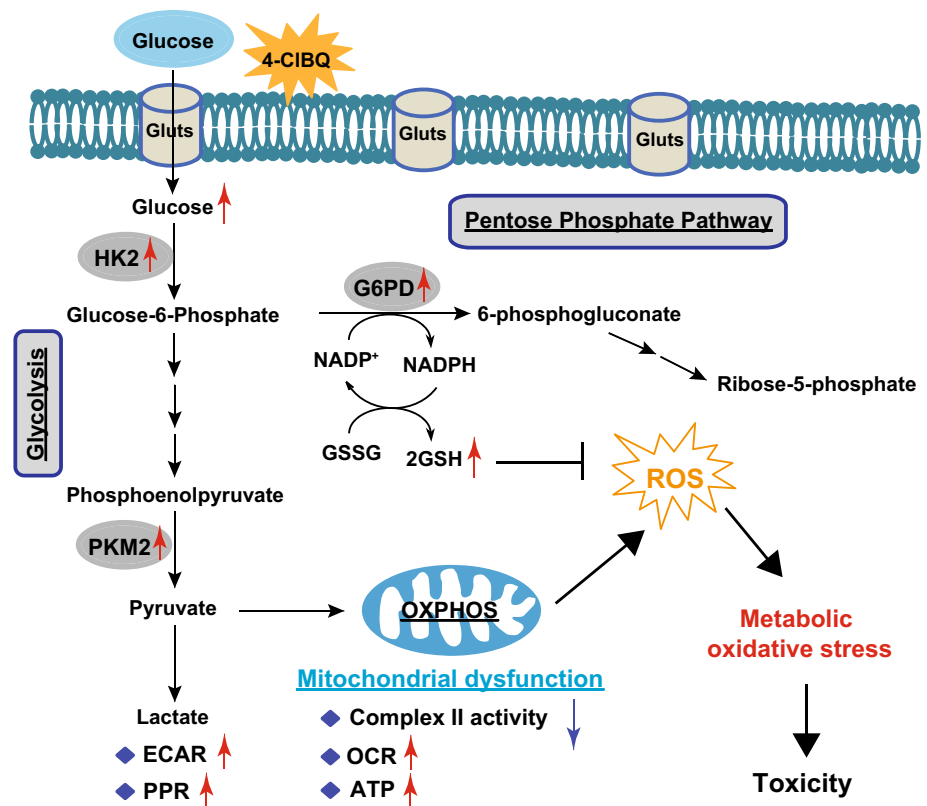


catalyzes the final step of glycolysis and converts phosphoenolpyruvate into pyruvate and ATP (Lunt and Vander Heiden 2011).

Because G6PD catalyzes the rate-limiting step of the pentose phosphate pathway that provides reducing equivalents to detoxify hydroperoxides, increase in *g6pd* expression is anticipated to increase cellular GSH levels. Indeed, a dose-dependent increase in cellular GSH levels was observed in 4-ClBQ-treated cells (Fig. 3a). To determine the biological significance of increases in *g6pd* expression, cells were treated with DHEA (inhibits G6PD activity) prior to the 4-ClBQ treatment and cell survival was measured using a clonogenic assay. Results showed that inhibiting G6PD activity augments 4-ClBQ-induced toxicity (Fig. 3b), suggesting that the protective function of the pentose phosphate pathway is functional in 4-ClBQ-treated HaCaT cells. These results are also consistent with literature reports demonstrating the protective role of the pentose phosphate pathway in response to oxidative stress (Cosentino et al. 2011; Filosa et al. 2003; Pandolfi et al. 1995; Salvemini et al. 1999; Tian et al. 1999; Tuttle et al. 2000; Ursini et al. 1997). Overexpression of *g6pd* has been shown to increase cellular GSH levels, which is associated with significant decreases in cellular ROS levels and toxicity in hydrogen peroxide-treated HeLa cells (Salvemini et al. 1999). Increases in *g6pd* expression have also been shown in hydrogen peroxide-treated human hepatoma HepG2 and

Hep3B cells as well as in human Jurkat T-cells (Ursini et al. 1997). Ionizing radiation treatment, a well-known ROS generating agent, increases G6PD activity, and siRNA-mediated inhibition of *g6pd* expression enhanced ionizing radiation-induced DNA damage in human fibroblasts (Cosentino et al. 2011). Pharmacological inhibition of G6PD activity using DHEA and 6-aminonicotinamide also sensitized rat PC12 cells to hydrogen peroxide-induced toxicity (Tian et al. 1999). *g6pd* knockout sensitized mouse embryonic stem cells and Chinese Hamster Ovary fibroblasts to chemical oxidant diamide and ionizing radiation-induced toxicity (Filosa et al. 2003; Pandolfi et al. 1995; Tuttle et al. 2000). These previously published results and results from this study (Fig. 3) demonstrate the protective function of the pentose phosphate pathway from toxicity induced by oxidative stress.

Previous studies report significant toxicity in 4-ClBQ-treated human keratinocytes and epithelial cells (Venkatesha et al. 2008; Xiao et al. 2013; Zhu et al. 2009). Because the protective property of the pentose phosphate pathway is functional in 4-ClBQ-treated HaCaT cells (Fig. 3), additional experiments were performed to determine whether mitochondrial function regulates toxicity in 4-ClBQ-treated cells. Initially, mitochondrial function was assessed by measuring OCR and levels of ATP. These results showed a dose-dependent increase in OCR and levels of ATP in 4-ClBQ-treated cells (Fig. 4a, b; Suppl. Figure 1c),

suggesting that the 4-ClBQ treatment perturbs mitochondrial (OXPHOS) function. The increase in OCR resulting in increases in ATP levels could be related to cellular response to combat 4-ClBQ-induced metabolic oxidative stress and toxicity.

Metabolic oxidative stress results from an imbalance between the steady-state levels of prooxidants (ROS: superoxide and hydrogen peroxide) and cellular antioxidant capacity that reduces these prooxidants. METC is believed to be one of the major metabolic sources of ROS (Boveris 1977). METC is composed of complex I–V. To investigate whether 4-ClBQ-induced metabolic oxidative stress and toxicity could result from changes in the activity of any one of these five METC complexes, a q-RT-PCR assay was performed to measure mRNA expression (Fig. 4c), and protein levels were measured using Western blotting (data not shown) of selected genes that regulate the activity of complex I (NADH dehydrogenase (ubiquinone) Fe–S protein 3, *ndufs3*), complex II (succinate dehydrogenase subunits A, B, C, and D; *sdha*, *sdhb*, *sdhc*, and *sdhd*), complex III (cytochrome C, *cytc*), complex IV (cytochrome c oxidase subunit IV and Va; *cox4*, *cox5a*), and complex V (ATP synthase beta and subunit 9; *atp5b*, *atp5g1*). Selection of these genes was based on the results obtained from the glucose metabolism PCR-array (data not shown) and literature reports. While the 4-ClBQ treatment did not affect the expression of the majority of the genes tested, a significant decrease in the mRNA expression of succinate dehydrogenase (complex II) subunit C and D (*sdhc* and *sdhd*) was observed (Fig. 4c). Results showed a dose-dependent decrease in the expression of *sdhc* and *sdhd* in 4-ClBQ-treated cells, while the same treatment did not affect the expression of *sdha* and *sdhb* (Fig. 5a). The mechanisms regulating the 4-ClBQ-induced down-regulation of the expression of *sdhc* and *sdhd* will be investigated in future studies. The decrease in the expression of *sdhc* and *sdhd* in 4-ClBQ-treated cells was also associated with approximately 60 % decrease in complex II activity (Fig. 5b). These results suggest that complex II activity could regulate metabolic oxidative stress and toxicity in 4-ClBQ-treated HaCaT cells.

Complex II consists of SDH subunits A, B, C, and D. All four subunits of complex II are nuclear encoded. Subunits A and B represent the hydrophilic head and catalytic core of complex II. They are localized in the mitochondrial matrix and convert succinate to fumarate releasing two electrons (Sun et al. 2005). The electrons are believed to passage through the flavin to the FeS-clusters and then to the coenzyme Q (CoQ)-binding site or the heme b site of SDHD (Slane et al. 2006; Sun et al. 2005). SDHC and SDHD are integral membrane proteins that are believed to anchor complex II into the mitochondria inner-membrane facilitating transfer of electrons to CoQ resulting in the reduction of ubiquinone into ubiquinol (Sun et al. 2005; Yankovskaya et al. 2003). Disruption of complex II activity in 4-ClBQ-treated cells due to a disproportionate subunit assembly (decrease in levels of SDHC and SDHD subunits) could result in increased accessibility of electrons to molecular oxygen dissolved in the membrane. This accessibility may facilitate the one-electron reduction of oxygen to superoxide, which could then dismute (spontaneously or enzymatically) to hydrogen peroxide resulting in an increase in the steady-state levels of ROS. 4-ClBQ-induced increases in the steady-state levels of ROS can initiate the Fenton chemistry to generate hydroxyl radicals leading to organic hydroperoxides that are capable of causing chronic oxidative stress and toxicity. Previously published results (Xiao et al. 2013) and results presented in this study are all consistent with this hypothesis. Our results are also consistent with earlier reports of PCB exposure negatively affecting the activity of METC complexes (Aly and Domenech 2009; Nishihara et al. 1986; Pardini 1971). The activity of complex I and II decreased approximately 80 % in isolated beef heart mitochondria treated with commercial PCB mixtures (Aroclor 1221, 1232, 1242, 1248, 1254, or 1260) (Pardini 1971). Aroclor 1254-induced decrease in complex I and III activity is associated with an increase in ROS generation, mitochondrial dysfunction and toxicity of hepatocytes (Aly and Domenech 2009). Tetrachlorobiphenyl (PCB95, 101, 107, or 109) treatment significantly inhibited the activity of complex II in isolated rat liver mitochondria (Nishihara et al. 1986). While the molecular mechanisms regulating the decrease in the activity of METC complexes are not completely understood, our results suggest that the 4-ClBQ-induced down-regulation of the expression of *sdhc* and *sdhd* negatively impacts complex II activity resulting in an increase in the steady-state levels of ROS. This increase in metabolic oxidative stress sensitizes HaCaT cells to 4-ClBQ-induced toxicity.

To further investigate the test of causality, experiments were repeated in HaCaT cells overexpressing *sdhc* and *sdhd* (Fig. 6). As anticipated, overexpression of *sdhc* and *sdhd* did not increase the basal activity of complex II (Fig. 6a–c). However, 4-ClBQ-induced decrease in complex II activity was suppressed in cells overexpressing *sdhc* and *sdhd* (Fig. 6c). Restoring complex II activity may minimize the accessibility of electrons to molecular oxygen, which is anticipated to suppress 4-ClBQ-induced increase in the steady-state levels of cellular ROS and toxicity. Indeed, results from flow cytometry measurements of cellular ROS levels did show a significant inhibition in 4-ClBQ-induced increase in the steady-state levels of cellular ROS (Fig. 6d, e). This inhibition in cellular ROS levels was associated with a significant protection of HaCaT cells from 4-ClBQ-induced toxicity (Fig. 6f). These results demonstrate the causality of complex II activity regulating

metabolic oxidative stress and toxicity in 4-ClBQ-treated HaCaT human keratinocytes.

In summary, these results demonstrate that the 4-ClBQ treatment induces metabolic oxidative stress and toxicity in HaCaT human keratinocytes. While the protective function of the pentose phosphate pathway is active in 4-ClBQ-treated cells, down-regulation of the expression of METC complex II subunit C and D (*sdhc* and *sdhd*) increases the steady-state levels of cellular ROS resulting in toxicity (Fig. 7). This basic science knowledge of PCB-induced metabolic oxidative stress (perturbation in glucose metabolism and OXPHOS) in human cells could be of significance in understanding the higher incidence of diabetes in the residents of Anniston, Alabama where PCBs were manufactured from 1929 to 1971 (Silverstone et al. 2012).

**Conflict of interest** The authors declare they have no actual or potential competing financial interests.

# References

Aly HA, Domenech O (2009) Aroclor 1254 induced cytotoxicity and mitochondrial dysfunction in isolated rat hepatocytes. Toxicology 262:175–183. doi:10.1016/j.tox.2009.05.018

Balaban RS, Nemoto S, Finkel T (2005) Mitochondria, oxidants, and aging. Cell 120:483–495. doi:10.1016/j.cell.2005.02.001

Boukamp P, Petrussevska RT, Breitkreutz D, Hornung J, Markham A, Fusenig NE (1988) Normal keratinization in a spontaneously immortalized aneuploid human keratinocyte cell line. J Cell Biol 106:761–771

Boveris A (1977) Mitochondrial production of superoxide radical and hydrogen peroxide. Adv Exp Med Biol 78:67–82

Cosentino C, Grieco D, Costanzo V (2011) ATM activates the pentose phosphate pathway promoting anti-oxidant defence and DNA repair. EMBO J 30:546–555. doi:10.1038/emboj.2010.330

Cossarizza A et al (2009) Simultaneous analysis of reactive oxygen species and reduced glutathione content in living cells by polychromatic flow cytometry. Nat Protoc 4:1790–1797. doi:10.1038/nprot.189

DeCaprio AP et al (2005) Polychlorinated biphenyl (PCB) exposure assessment by multivariate statistical analysis of serum congener profiles in an adult Native American population. Environ Res 98:284–302. doi:10.1016/j.envres.2004.09.004

Filosa S et al (2003) Failure to increase glucose consumption through the pentose-phosphate pathway results in the death of glucose-6-phosphate dehydrogenase gene-deleted mouse embryonic stem cells subjected to oxidative stress. Biochem J 370:935–943. doi:10.1042/bj20021614

Hansen LG, DeCaprio AP, Nisbet ICT (2003) PCB congener comparisons reveal exposure histories for residents of Anniston, Alabama, USA. Fresenius Environ Bull 12:181–190

Herrick RF, Lefkowitz DJ, Weymouth GA (2007) Soil contamination from PCB-containing buildings. Environ Health Perspect 115:173–175. doi:10.1289/ehp.9646

Herrick RF, Meeker JD, Altshul L (2011) Serum PCB levels and congener profiles among teachers in PCB-containing schools: a pilot study. Environ Health 10:56–66. doi:10.1186/1476-069x-10-56

Hu D, Hornbuckle KC (2009) Inadvertent polychlorinated biphenyls in commercial paint pigments. Environ Sci Technol 44:2822–2827. doi:10.1021/es902413k

Hu D, Lehmler HJ, Martinez A, Wang K (2010) Hornbuckle KC (2010) Atmospheric PCB congeners across Chicago. Atmos Environ 44:1550–1557. doi:10.1016/j.atmosenv.01.006

Lauby-Secretan B et al (2013) Carcinogenicity of polychlorinated biphenyls and poly-brominated biphenyls. Lancet Oncol 14:287–288. doi:10.1016/s1470-2045(13)70104-9

Lehmler HJ, Robertson LW (2001) Synthesis of polychlorinated biphenyls (PCBs) using the Suzuki-coupling. Chemosphere 45:137–143

Liebl B, Schettgen T, Kerscher G, Broding HC, Otto A, Angerer J, Drexler H (2004) Evidence for increased internal exposure to lower chlorinated polychlorinated biphenyls (PCB) in pupils attending a contaminated school. Int J Hyg Environ Health 207:315–324. doi:10.1078/1438-4639-00296

Lunt SY, Vander Heiden MG (2011) Aerobic glycolysis: meeting the metabolic requirements of cell proliferation. Annu Rev Cell Dev Biol 27:441–464. doi:10.1146/annurev-cellbio-092910-154237

Martinez A, Erdman NR, Rodenburg ZL, Eastling PM, Hornbuckle KC (2012) Spatial distribution of chlordanes and PCB congeners in soil in Cedar Rapids, Iowa, USA. Environ Pollut 161:222–228. doi:10.1016/j.envpol.2011.10.028

McLean MR, Bauer U, Amaro AR, Robertson LW (1996) Identification of catechol and hydroquinone metabolites of 4-monochlorobiphenyl. Chem Res Toxicol 9:158–164. doi:10.1021/tx950083a

Nishihara Y, Robertson LW, Oesch F, Utsumi K (1986) The effects of tetrachlorobiphenyls on the electron transfer reaction of isolated rat liver mitochondria. Life Sci 38:627–635

Pandolfi PP, Sonati F, Rivi R, Mason P, Grosveld F, Luzzatto L (1995) Targeted disruption of the housekeeping gene encoding glucose 6-phosphate dehydrogenase (G6PD): G6PD is dispensable for pentose synthesis but essential for defense against oxidative stress. EMBO J 14:5209–5215

Pardini RS (1971) Polychlorinated biphenyls (PCB): effect on mitochondrial enzyme systems. Bull Environ Contam Toxicol 6:539–545

Ross G (2004) The public health implications of polychlorinated biphenyls (PCBs) in the environment. Ecotoxicol Environ Saf 59:275–291. doi:10.1016/j.ecoenv.2004.06.003

Safe S (1993) Toxicology, structure-function relationship, and human and environmental health impacts of polychlorinated biphenyls: progress and problems. Environ Health Perspect 100:259–268

Salvemini F, Franze A, Iervolino A, Filosa S, Salzano S, Ursini MV (1999) Enhanced glutathione levels and oxidoresistance mediated by increased glucose-6-phosphate dehydrogenase expression. J Biol Chem 274:2750–2757

Silverstone AE, Rosenbaum PF, Weinstock RS, Bartell SM, Foushee HR, Shelton C, Pavuk M (2012) Polychlorinated biphenyl (PCB) exposure and diabetes: results from the Anniston Community Health Survey. Environ Health Perspect 120:727–732. doi:10.1289/ehp.1104247

Slane BG, Aykin-Burns N, Smith BJ, Kalen AL, Goswami PC, Domann FE, Spitz DR (2006) Mutation of succinate dehydrogenase subunit C results in increased $O_2^-$, oxidative